Hindawi
Mathematical Problems in Engineering
Volume 2018, Article ID 9373468, 8 pages
https://doi.org/10.1155/2018/9373468

Research Article

Performance Analysis of CDMA/ALOHA Networks in Memory Impulse Channels

Shu-Ming Tseng,[1] Yung-Chung Wang,[2] Cheng-Wei Hu,[2] and Tseng-Chun Lee[1]

[1] *Department of Electronic Engineering, National Taipei University of Technology, No. 1, Sec. 3, Zhongxiao E. Rd., Taipei 10608, Taiwan*
[2] *Department of Electrical Engineering, National Taipei University of Technology, No. 1, Sec. 3, Zhongxiao E. Rd., Taipei 10608, Taiwan*

Correspondence should be addressed to Yung-Chung Wang; ycwang@ntut.edu.tw

Received 2 January 2018; Accepted 13 May 2018; Published 7 June 2018

Academic Editor: Filippo Cacace

Previous CDMA/ALOHA network performance analysis papers do not consider memory impulse channels. The Markov-Gaussian model can characterize the bursty nature of the memory impulsive noise in some wireless channels and power line communication (PLC) channels. In this paper, we propose the use of the Markov-Gaussian model in the throughput analysis of CDMA/ALOHA networks. The state transition diagram for the throughput analysis has one extra dimension to represent if the impulse noise is present or not. We derive the exact throughput analysis in memory impulse channels with and without channel load sensing protocol (CLSP). The analytic results demonstrate that if the level of the impulsive noise is higher, performance degradation is more and vice versa. Based on the analytic results, we also find the optimal CLSP threshold alpha for various impulse noise conditions. The analytic results of the throughput performance are all matched by the simulation results.

1. Introduction

Code division multiple access (CDMA) is popular in wireless networks and power line communication (PLC) networks [1–7]. ALOHA is a popular media access control (MAC) protocol in wireless and PLC networks [8, 9]. The performance of the CDMA/ALOHA networks has been analyzed in wireless communication systems [10–14], RFID systems [15], neighbor discovery in wireless networks [16], and satellite communications [17, 18]. However, these previous studies considered only memoryless thermal noise (additive white Gaussian noise) and did not consider the memory impulse noise.

Impulse noise occurs in indoor wireless networks [19], industrial wireless sensor networks [20, 21], and PLC networks [22, 23]. The source of memory impulse noise includes printers, cash registers, microwave ovens [19], motors, ignition systems, heavy machineries, and electric switch [21]. They are often described by Middleton Class A model [24] or Bernoulli-Gaussian model [25]. However, these models are memoryless, so the bursty nature of the memory impulse noise for several consecutive samples cannot be represented [22]. Markov chains are therefore used to modify the two aforementioned memory models. The Markov-Middleton model [26] is based on the Middleton Class A model and the Markov-Gaussian model [21, 23, 27, 28] is based on the Bernoulli-Gaussian model [29].

In this paper, we propose to apply the Markov-Gaussian channel to model the memory impulse noise and then analyze the throughput of the CDMA/ALOHA networks. The Markov-Gaussian channel adds one extra dimension to the state transition diagram in the previous papers about performance analysis of the CDMA/ALOHA networks. Additionally, we consider the channel load sensing protocol (CLSP) [10, 30]. In CLSP, the base station or access point measures the number of transmitting users; this is defined as the channel load. If the number of transmitting users is smaller than a certain value, we allow the packet transmission. Otherwise, we deny the transmission of the packet. The advantage of CLSP is that it can improve the throughput in high offered load.

The contributions of this paper are as follows:

(1) Based on the Markov-Gaussian channel and the two-dimensional state transition diagram with one extra dimension representing the memory impulse

noise, we derive the exact throughput analysis of the CDMA/ALOHA network without CLSP and with CLSP in memory impulse channels. In the throughput analysis equations, the additional summation over j represents the extra dimension of the memory impulse noise state, and additional multiplicative term $h_{j',j}$ represents the state transition of the memory impulse noise from state j' to state j. The summation over $j = 1,2$; thus, the complexity is doubled. These do not exist in previous papers [10–12], which considered only memoryless thermal noise.

(2) Based on the throughput analysis results, we determine the optimal CLSP threshold for various impulse noise conditions.

The remainder of this paper is organized as follows. In Section 2, the Markov-Gaussian channel model is introduced. We describe system model in Section 3. The throughput analysis in the Markov-Gaussian channel without CLSP is presented in Section 4. In Section 5, the throughput with CLSP is analyzed. In Section 6, we present the numerical results of the throughput analysis without and with CLSP. The conclusion is presented in Section 7.

2. Markov-Gaussian Channel Model

The Markov-Gaussian channel model [27] is a hybrid Markov chain with two states to model memory (bursty) impulse noise. The channel state $j = 1$ represents the Gaussian noise only, and the channel state $j = 2$ represents the impulse noise. The Markov-Gaussian channel model provides a simple method to describe the bursty nature of the channel state. First, the received signal at time index l is

$$y_l = x_l + n_l, \tag{1}$$

where x_l is the transmitted signal and has the bit energy E_b and n_l is the noise. Then, the probability density functions (PDF) of n_l are as follows:

$$P(n_l \mid j = 1) = \frac{1}{\sqrt{2\pi\sigma_G^2}} \exp\left\{-\frac{|n_l|^2}{2\sigma_G^2}\right\} \tag{2}$$

$$P(n_l \mid j = 2) = \frac{1}{\sqrt{2\pi R\sigma_G^2}} \exp\left\{-\frac{|n_l|^2}{2R\sigma_G^2}\right\} \tag{3}$$

where σ_G^2 denotes the Gaussian noise variance and R denotes the average noise ratio between the impulse noise and the Gaussian noise and R>>1. The channel state transition probabilities can be written as follows:

$$h_{MN} = P\left(j'' = N \mid j = M\right) \quad M, N = \{1, 2\} \tag{4}$$

where j'' is the next state.

Therefore, the state probabilities can be replaced as follows:

$$P_1 = P(j = 1) = \frac{h_{21}}{h_{12} + h_{21}} \tag{5}$$

$$P_2 = P(j = 2) = \frac{h_{12}}{h_{12} + h_{21}} \tag{6}$$

We define the channel state transition probability matrix $\mathbf{H}$ as follows:

$$\mathbf{H} = \begin{bmatrix} h_{11} & h_{12} \\ h_{21} & h_{22} \end{bmatrix} \tag{7}$$

The channel memory parameter ω is defined as [31]

$$\omega = \frac{1}{h_{12} + h_{21}} \tag{8}$$

When ω=1, the channel is memoryless. When $\omega > 1$, the channel has a persistent memory. The rationale is presented in the Appendix. In this study, we consider $\omega > 1$, a persistent memory channel.

3. System Model

A CDMA/ALOHA network with memory (bursty) impulse noise is considered. Let N denote the CDMA processing gain and L denote the packet length in bits. We assume one hub station and infinitely many users. We denote G (packet/packet duration) as the offered load and S (packet/packet duration) as the $T_p = L/\gamma$ throughput. (sec) is the packet duration, where γ is the data rate (bits/sec).

We assume a CDMA system with k interfering users, because of memory impulse noise. The bit error probabilities P_b for the Gaussian noise (j=1) are given by [10–12]

$$\begin{aligned} P_b(k, j = 1) &= \frac{2}{3} Q\left[\left(\frac{k}{3N} + \frac{N_0}{2E_b}\right)^{-0.5}\right] \\ &\quad + \frac{1}{6} Q\left[\left(\frac{k\left(N/3 + \sqrt{3}\sigma\right)}{N^2} + \frac{N_0}{2E_b}\right)^{-0.5}\right] \\ &\quad + \frac{1}{6} Q\left[\left(\frac{k\left(N/3 - \sqrt{3}\sigma\right)}{N^2} + \frac{N_0}{2E_b}\right)^{-0.5}\right] \end{aligned} \tag{9}$$

Note the enlarged noise variance $R\sigma_G^2$ in (3), and we obtain the bit error probabilities P_b for impulse noise ($j = 2$) as follows:

$$\begin{aligned} P_b(k, j = 2) &= \frac{2}{3}Q\left[\left(\frac{k}{3N} + \frac{RN_0}{2E_b}\right)^{-0.5}\right] \\ &+ \frac{1}{6}Q\left[\left(\frac{k\left(N/3 + \sqrt{3}\sigma\right)}{N^2} + \frac{RN_0}{2E_b}\right)^{-0.5}\right] \\ &+ \frac{1}{6}Q\left[\left(\frac{k\left(N/3 - \sqrt{3}\sigma\right)}{N^2} + \frac{RN_0}{2E_b}\right)^{-0.5}\right] \end{aligned} \tag{10}$$

where

$$\sigma^2 = k\left[N^2\frac{23}{360} + N\left(\frac{1}{20} + \frac{k-1}{36}\right) - \frac{1}{20} - \frac{k-1}{36}\right] \tag{11}$$

and $N_0/2$ denotes the noise power spectral density and $Q(x)$ is defined as

$$Q(x) = \frac{1}{\sqrt{2\pi}}\int_x^{\infty}\exp\left(-\frac{u^2}{2}\right)du \tag{12}$$

4. Throughput Analysis for CDMA/ALOHA Network in Markov-Gaussian Channel without CLSP

We use the $M/M/\infty$ queuing models to model the CDMA/ALOHA networks with fixed packet length [11, 12]. The validity of the $M/M/\infty$ queuing model, as stated in [11, 12], is justified as follows. Theorem 4.1 in [32] shows that the number of users in M/G/∞ queuing system is a function of the *mean* of the packet length only, not the *distribution* of the packet length. Thus, M/M/∞ (exponential packet length) is equal to M/D/∞ (fixed packet length) in CDMA/Unslotted ALOHA throughput analysis because the bit error probability (and thus packet success probability) depends on the number of users only, as shown in (9) and (10).

First, we define the steady state probability $P_{k,j}$ which is the probability that there are k interfering packets and the state is j on the 1st bit.

$$P_{k,j} = P_j e^{-(\lambda/\mu)}\frac{(\lambda/\mu)^k}{k!}, \quad k \geq 0, \ j = \{1, 2\}, \tag{13}$$

where P_j is the state probabilities defined in (5) and (6) and μ is the death rate defined as

$$\mu = \frac{k}{T_p} \tag{14}$$

Furthermore, λ is the arrival rate defined as

$$\lambda = \frac{G}{T_p} \tag{15}$$

$P_s(k, j, i)$ is defined as the probability that there are k interfering packets, and on the i-th bit the Markov-Gaussian channel is in the state j and the first (i-1) bits are all correct. The state transition diagram in Markov-Gaussian channels is shown in Figure 1. The Markov-Gaussian channels introduce an additional dimension j=1 or 2, compared to previous CDMA/ALOHA throughput analysis papers.

The initial condition $P_s(k, j, 1)$ is a

$$P_s(k, j, 1) = P_{k,j}, \quad k = 0, 1, 2\ldots, \ j = \{1, 2\}. \tag{16}$$

We can recursively derive $P_s(k, j, i)$ by

$$\begin{aligned} P_s(k, j, i) = \sum_{j'=1}^{2}\Big[&(1 - \lambda\Delta t - k\mu\Delta t)\cdot P_s(k, j', i-1) \\ &\cdot\left(1 - P_b(k, j')\right)\cdot h_{j',j} + ((k+1)\mu\Delta t) \\ &\cdot P_s(k+1, j', i-1)\cdot\left(1 - P_b(k+1, j')\right)\cdot h_{j',j} \\ &+ (\lambda\Delta t)\cdot P_s(k-1, j', i-1)\cdot\left(1 - P_b(k-1, j')\right) \\ &\cdot h_{j',j}\Big] \end{aligned} \tag{17}$$

where j' is the state in the i-1_{th} bit. Note that summation over j represents one extra dimension and $h_{j',j}$ represent the state transition of the memory impulse noise from j' to j. These did not exist in the previous CDMA/ALOHA throughput analysis papers [10–12] because they did not consider memory impulse noise.

From (16) and recursive form of (17), we can obtain $P_s(k, j, 2)$, $P_s(k, j, 3)$, and finally $P_s(k, j, L)$.

Then, we obtain the packet success probability Q_s

$$Q_s = \sum_{j=1}^{2}\sum_{k=0}^{\infty}\{(1 - P_b(k, j))P_s(k, j, L)\} \tag{18}$$

Finally, we obtain the throughput S

$$S = G \times Q_s \tag{19}$$

5. Throughput Analysis in Markov-Gaussian Channels with CLSP

The channel load sensing protocol (CLSP) allows packet transmission when the current number of users is smaller than the threshold α and denies packet transmissions otherwise. Therefore, the maximum number of transmitting packets is α.

Next, we define $P_{sclsp}(k, j, i)$ as the probability that there are k interfering packets and at the i-th bit; the Markov-Gaussian channel is in the state j and the first (i-1) bits are all correct. The state transition diagram of the CDMA/ALOHA networks with CLSP in Markov-Gaussian channels is shown in Figure 2. The Markov-Gaussian channels introduce an additional dimension j=1 or 2, compared

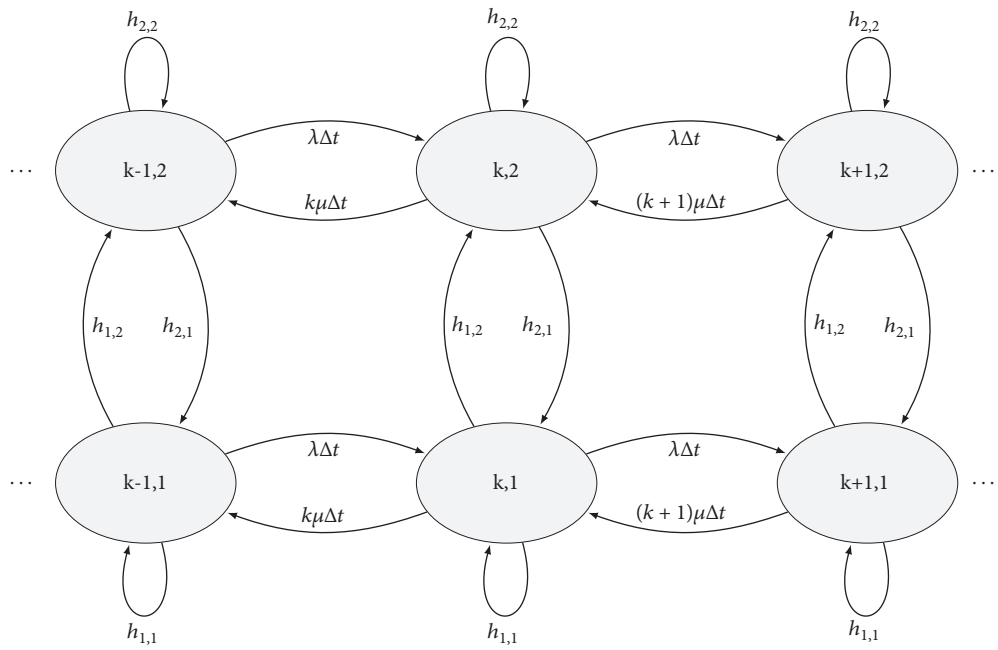

Figure 1: Two-dimensional state transition diagram in Markov-Gaussian channels.

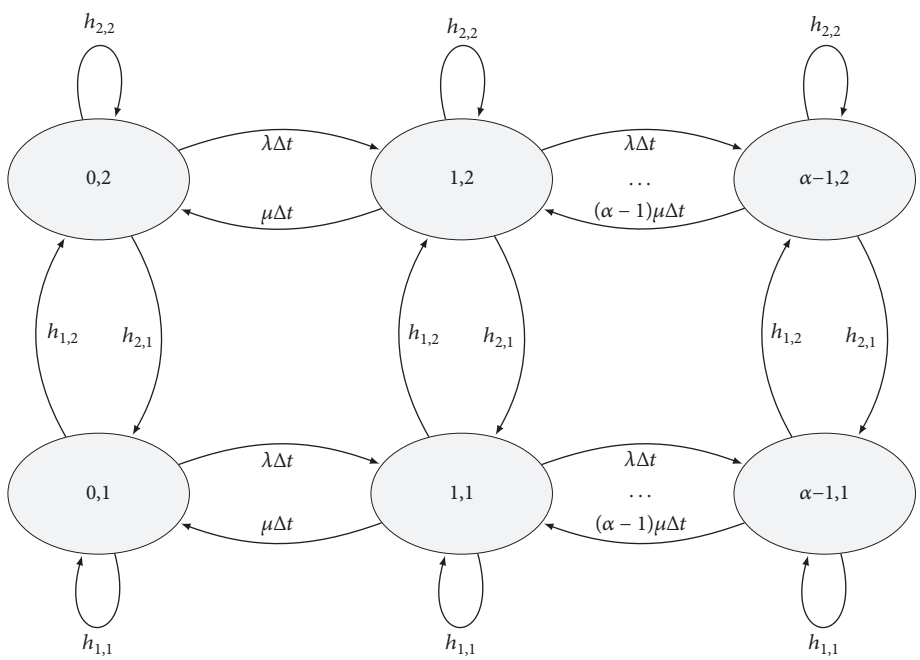

Figure 2: Two-dimensional state transition diagram with CLSP in Markov-Gaussian channels.

to previous CDMA/ALOHA throughput analysis papers. Figures 1 and 2 are different because the maximum interfering packets are limited to α-1 owing to CLSP in Figure 2.

The initial condition $P_{sclsp}(k, j, 1)$ is as follows:

$$P_{sclsp}(k, j, 1) = \frac{P_s(k, j, 1)}{\sum_{k=0}^{\alpha-1} P_s(k, j, 1)}. \tag{20}$$

Further, we derive $P_{sclsp}(k, j, i)$ in recursive form

$$\begin{aligned} P_{sclsp}(k, j, i) = \sum_{j'=1}^{2} \Big[& (1 - \lambda\Delta t - k\mu\Delta t) \\ & \cdot P_{sclsp}(k, j', i-1) \cdot \left(1 - P_b(k, j')\right) \cdot h_{j',j} + (\lambda\Delta t) \\ & \cdot P_{sclsp}(k-1, j', i-1) \cdot \left(1 - P_b(k-1, j')\right) \cdot h_{j',j} \end{aligned}$$

$$+\left((k+1)\,\mu\Delta t\right)\cdot P_{sclsp}\left(k+1, j', i-1\right)$$
$$\cdot\left(1-P_b\left(k+1, j'\right)\right)\cdot h_{j',j}\Big] \tag{21}$$

where j' is the state in the i-1_{th} bit. Note that summation over j represents one extra dimension and $h_{j',j}$ represent the state transition of the memory impulse noise from j' to j. These do not exist in the previous CDMA/ALOHA throughput analysis papers [10–12] because they do not consider memory impulse noise.

We obtain the packet success probability Q_{clsp}

$$Q_{clsp}=\sum_{j=1}^{2}\sum_{k=0}^{\alpha-1}\left\{\left(1-P_b\left(k,j\right)\right)P_{sclsp}\left(k,j,L\right)\right\} \tag{22}$$

We compute the throughput S_{clsp} as

$$S_{clsp}=G_{clsp}\times Q_{clsp} \tag{23}$$

where we define G_{clsp} as the mean offered load given by

$$G_{clsp}=\frac{\sum_{k=0}^{\alpha-1}k\cdot P_s\left(k,j,1\right)}{\sum_{k=0}^{\alpha-1}P_s\left(k,j,1\right)} \tag{24}$$

6. Numerical Results

The system parameters are the same as [10–12] to facilitate comparisons. The packet length L = 1,000 bits, SNR = 30 dB, processing gain N = 30, and the data rate γ= 9.6 kbps. The channel memory parameter ω=10, and the state probability P_2=0.1 [27]. The channel state transition probability matrix **H** is given in (25), and the average noise ratio between impulse noise and Gaussian noise, R = 10 and R = 100; these parameters are the same as [27, 28].

$$\mathbf{H}=\begin{bmatrix}0.99 & 0.01\\ 0.09 & 0.91\end{bmatrix} \tag{25}$$

In Figure 3, we compare the throughput in Markov-Gaussian channels for R=1-150, where R=1 represents the case of no impulse noise (Gaussian noise only). We observe that the network throughput is worse when the impulse noise is larger (R is larger). For example, the peak throughput S= 4.21 when the offered load G=6 for R=1, and the peak throughput S= 3.14 when offered load G=6 for R=150. The analytic results in lines and the simulated results in symbols are close; thus, the accuracy of the throughput analysis is confirmed.

In Figures 4 and 5, we present the analytic throughput (in lines) and simulated throughput (in symbols) in Markov-Gaussian channels with CLSP for R=10.

In Figures 6 and 7, we present the analytic throughput (in lines) and simulated throughput (in symbols) in Markov-Gaussian Model with CLSP for R=150.

According to Figures 4–7, if α is too small, the packet will be refused transmissions. If α is too large, the multiple access interference (MAI) of CDMA systems is more severe, so the throughput gets worse. When the offered load is high, the

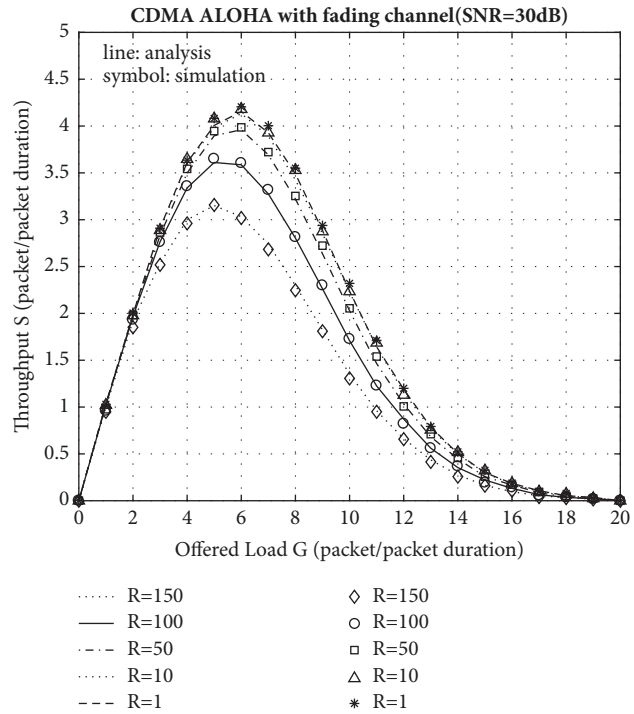

Figure 3: Simulation and numerical results of the throughput for various R.

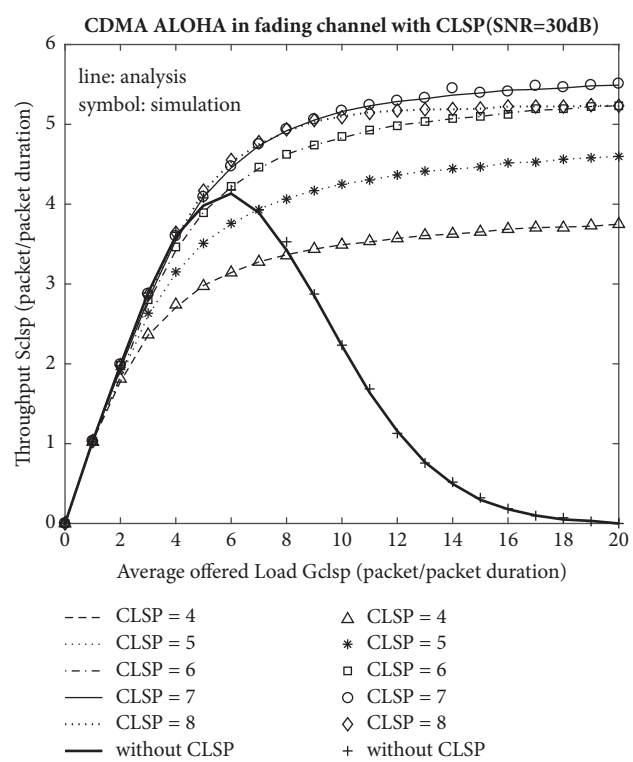

Figure 4: Throughput for R=10 with CLSP ($\alpha \leq 8$).

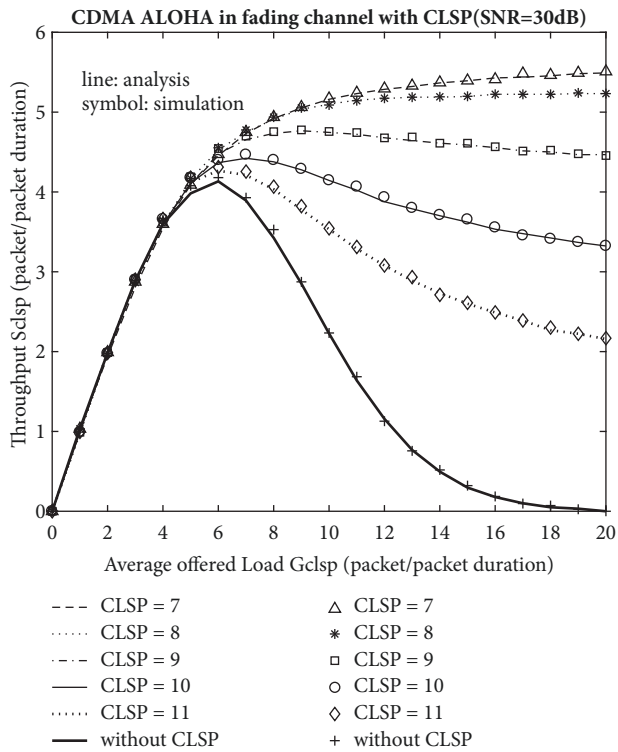

Figure 5: Throughput for R=10 with CLSP ($\alpha \geq 7$).

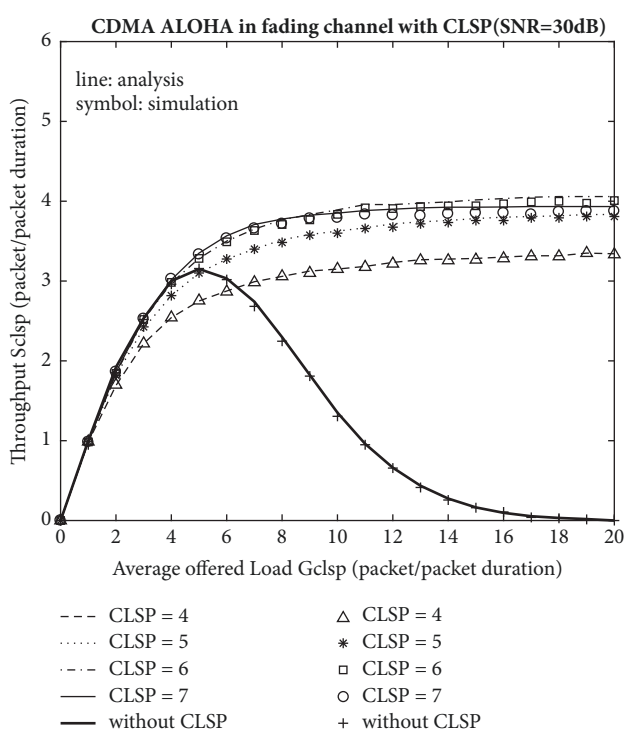

Figure 6: Throughput for R=150 with CLSP ($\alpha \leq 7$).

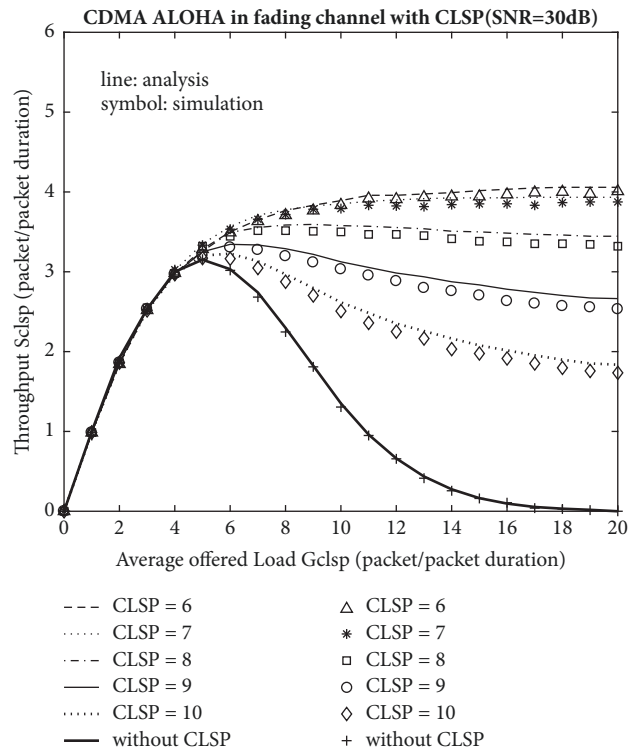

Figure 7: Throughput for R=150 with CLSP ($\alpha \geq 6$).

Table 1: Optimal CLSP threshold for different R.

average noise ratio R	threshold α
1	7
10	7
50	7
100	7
150	6

CLSP can reduce the MAI, so the throughput is higher than that without CLSP. In Figures 4 and 5, we find the optimum throughput when $\alpha = 7$ for R=10, and in Figures 6 and 7, we find the optimum throughput when $\alpha = 6$ for R=150. All the optimal CLSP thresholds α for R=1-150 are given in Table 1. We note that the optimal CLSP threshold α becomes smaller when R=150. This can be explained as follows: a larger impulse noise (R=150) increases the packet error rate and thus decreases the number of users allowed in the CLSP system.

Finally, in Figure 8 we compare the throughput in Markov-Gaussian channels with CLSP and the same threshold $\alpha = 7$ for R=1-150. We can see that, for the same CLSP threshold α, the system with CLSP throughput is smaller, when the impulse noise is larger (R is larger).

For example, the throughput S_{clsp}= 5.5 when offered load G_{clsp}=20 for R=1, and the throughput S_{clsp}= 3.9 when offered load G_{clsp}=20 for R=150.

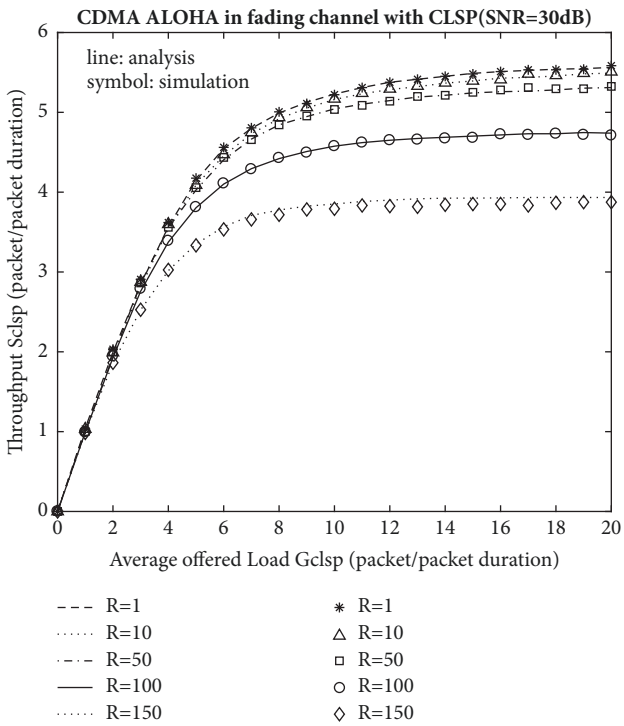

Figure 8: Throughput performance with CLSP ($\alpha = 7$).

7. Conclusions

In the study, we analyzed the CDMA/ALOHA network in Markov-Gaussian channels to characterize the bursty nature of the impulse noise. The previous papers about CDMA/ALOHA network did not consider memory impulse noise. The state transition diagram in Markov-Gaussian channels has one extra dimension representing whether the impulse noise is present or not. In the throughput analysis, the additional summation over j represents one extra dimension and additional $h_{j',j}$ represents the state transition of the memory impulse noise from j' to j. These were not presented in previous papers [10–12].

We derived the exact throughput analysis based on M/M/∞ queuing model without CLSP and with CLSP. In addition, based on the analytic results, we found the optimal CLSP threshold α for various R (the average noise ratio between the impulse noise and the Gaussian noise). The optimal CLSP threshold α for R=150 (large impulse noise) was smaller than that for R=1 (no impulse noise). We also found that the throughput is smaller when R is larger. For CLSP threshold $\alpha = 7$ and offered load G=20, the peak throughput decreased from 5.5 to 3.9 when R increased from 1 (no impulse noise) to 150 (large impulse noise).

Appendix

In Section 2, we define the parameter ω to determine channel memory. When $\omega = 1$, the channel is memoryless, and when $\omega > 1$, the channel has persistent memory. In the following section, we prove that this result is correct.

There are two cases. One is memoryless and in the other, the channel has a persistent memory. In the first case, we define the state probability $P_2 = 0.1$ and $\omega = 1$ [27]. In the second case, the state probability is defined as $P_2 = 0.1$ and $\omega = 10$ [27]. Then, we use (6) and (8) to obtain the channel state transition probability matrix **H**. Their calculation processes are as follows.

Case 1.

$$\begin{cases} P_2 = 0.1 = \dfrac{h_{12}}{h_{12} + h_{21}} \\ \omega = 1 = \dfrac{1}{h_{12} + h_{21}} \end{cases} \longrightarrow \tag{A.1}$$

$$H = \begin{bmatrix} h_{11} & h_{12} \\ h_{21} & h_{22} \end{bmatrix} = \begin{bmatrix} 0.9 & 0.1 \\ 0.9 & 0.1 \end{bmatrix}$$

Case 2.

$$\begin{cases} P_2 = 0.1 = \dfrac{h_{12}}{h_{12} + h_{21}} \\ \omega = 10 = \dfrac{1}{h_{12} + h_{21}} \end{cases} \longrightarrow \tag{A.2}$$

$$H = \begin{bmatrix} h_{11} & h_{12} \\ h_{21} & h_{22} \end{bmatrix} = \begin{bmatrix} 0.99 & 0.01 \\ 0.09 & 0.91 \end{bmatrix}$$

According to the channel state transition probability matrix H of the two cases, the channel state transition probability h_{11} is the same as h_{21} and h_{12} is the same as h_{22} in Case 1; therefore, Case 1 is memoryless. Furthermore, in Case 2, h_{11} is not the same as h_{21} and h_{12} is not the same as h_{22}; therefore, Case 2 has persistent memory.

Data Availability

The data used to support the findings of this study are available from the corresponding author upon request.

Conflicts of Interest

The authors declare that they have no conflicts of interest.

Acknowledgments

This work was supported in part by Ministry of Science and Technology, Taiwan, under Grant MOST 105-2221-E-027-007.

References

[1] W.-J. Huang, W.-W. Hu, C.-P. Li, and J.-C. Chen, "Novel metric-based PAPR reduction schemes for MC-CDMA systems," *IEEE Transactions on Vehicular Technology*, vol. 64, no. 9, pp. 3982–3989, 2015.

[2] Z. Wang, D. Yang, and L. B. Milstein, "Multi-user resource allocation for a distributed multi-carrier DS-CDMA network," *IEEE Transactions on Communications*, vol. 60, no. 1, pp. 143–152, 2012.

[3] Y.-C. Tseng, C.-M. Chao, and S.-L. Wu, "Code placement and replacement strategies for wideband CDMA OVSF code tree management," in *Proceedings of the IEEE Global Telecommunications Conference, GLOBECOM '01.*, vol. 1, pp. 562–566, San Antonio, TX, USA, 2001.

[4] E. Vahedi, R. K. Ward, and I. F. Blake, "Performance analysis of RFID protocols: CDMA versus the standard EPC Gen-2," *IEEE Transactions on Automation Science and Engineering*, vol. 11, no. 4, pp. 1250–1261, 2014.

[5] F. Z. Doudou and A. Djebbari, "Particle swarm optimization aided serial acquisition in distributed OSCFAR and CMLD for DS-CDMA systems in fading channels," *Wireless Personal Communications*, vol. 94, no. 3, pp. 621–640, 2017.

[6] Y. Liang, X. Da, and S. Wang, "On narrowband interference suppression in OFDM-based systems with CDMA and weighted-type fractional fourier transform domain preprocessing," *KSII Transactions on Internet and Information Systems*, vol. 11, no. 11, pp. 5377–5391, 2017.

[7] H. Nosato, Y. Kasai, E. Takahashi, and M. Murakawa, "A very low-cost low-frequency PLC system based on DS-CDMA for DC power lines," in *Proceedings of the 2012 16th IEEE International Symposium on Power Line Communications and Its Applications, ISPLC 2012*, pp. 398–403, IEEE, Beijing, China, March 2012.

[8] I. B. Arun and T. G. Venkatesh, "Order statistics based analysis of pure ALOHA in channels with multipacket reception," *IEEE Communications Letters*, vol. 17, no. 10, pp. 2012–2015, 2013.

[9] X. Zheng, Y. Zhen, and G. Weng, "The simulation using OPNET for MAC protocol of power line network," *Journal of Zhejiang University of Technology*, vol. 40, no. 1, 2012.

[10] S.-M. Tseng, "A high-throughput multicarrier DS CDMA/ALOHA network," *IEICE Transactions on Communications*, vol. E86-B, no. 4, pp. 1265–1273, 2003.

[11] S.-M. Tseng, H.-P. Lin, C.-H. Chen, and Y.-C. Wang, "Throughput analysis of DS CDMA/unslotted ALOHA wireless networks with fixed packet length in rayleigh fading finite-state markov channel model," *Wireless Personal Communications*, vol. 71, no. 4, pp. 3091–3104, 2013.

[12] S.-M. Tseng, L.-H. Chiang, and Y.-C. Wang, "Throughput of coded CDMA/ALOHA networks with variable length data traffic and two user classes in rayleigh fading FSMC mode," *KSII Transactions on Internet and Information Systems*, vol. 8, no. 12, pp. 4324–4342, 2014.

[13] H. Saragih and F. Santoso, "Differential maximum ratio combining (MRC)-based throughput analysis on dual-fading models of Slotted-ALOHA CDMA systems," *International Journal of Wireless Information Networks*, vol. 21, no. 2, pp. 154–160, 2014.

[14] I. Lim, "Slotted random access protocol with dynamic transmission probability control in CDMA system," *International Journal of Recent Trends in Engineering & Research*, vol. 2, no. 3, pp. 124–130, 2016.

[15] C. T. Nguyen, T. C. Thang, and A. T. Pham, "Performance analysis of hybrid ALOHA/CDMA anti-collision scheme for RFID systems over fading channels," in *Proceedings of the 7th International Conference on Ubiquitous and Future Networks, ICUFN 2015*, pp. 657–661, IEEE, Sapporo, Japan, July 2015.

[16] A. Russell, S. Vasudevan, B. Wang, W. Zeng, X. Chen, and W. Wei, "Neighbor discovery in wireless networks with multipacket reception," *IEEE Transactions on Parallel and Distributed Systems*, vol. 26, no. 7, pp. 1984–1998, 2015.

[17] G. Gallinaro, N. Alagha, R. De Gaudenzi, K. Kansanen, R. Muller, and P. Salvo Rossi, "ME-SSA: An advanced random access for the satellite return channel," in *Proceedings of the 2015 IEEE International Conference on Signal Processing for Communications (ICC)*, pp. 856–861, London, June 2015.

[18] K. Ohya, T. Takahashi, S. Kameda et al., "Efficient random access control scheme with reservation channel for QZSS short message SS-CDMA communication," in *Proceedings of the 2016 IEEE Wireless Communications and Networking Conference, WCNC 2016*, IEEE, Doha, Qatar, April 2016.

[19] K. L. Blackard, T. S. Rappaport, and C. W. Bostian, "Measurements and models of radio frequency impulsive noise for indoor wireless communications," *IEEE Journal on Selected Areas in Communications*, vol. 11, no. 7, pp. 991–1001, 1993.

[20] V. C. Gungor and G. P. Hancke, "Industrial wireless sensor networks: challenges, design principles, and technical approaches," *IEEE Transactions on Industrial Electronics*, vol. 56, no. 10, pp. 4258–4265, 2009.

[21] M. Cheffena, "Industrial wireless sensor networks: channel modeling and performance evaluation," *EURASIP Journal on Wireless Communications and Networking*, vol. 297, 2012.

[22] M. Zimmermann and K. Dostert, "Analysis and modeling of impulsive noise in broad-band powerline communications," *IEEE Transactions on Electromagnetic Compatibility*, vol. 44, no. 1, pp. 249–258, 2002.

[23] D.-F. Tseng, F. G. Mengistu, Y. S. Han, M. A. Mulatu, L.-C. Chang, and T.-R. Tsai, "Robust turbo decoding in a Markov Gaussian channel," *IEEE Wireless Communications Letters*, vol. 3, no. 6, pp. 633–636, 2014.

[24] D. Middleton, "Statistical-physical model of electromagnetic interference," *IEEE Transactions on Electromagnetic Compatibility*, vol. EMC-19, no. 3, pp. 106–126, 1977.

[25] M. Ghosh, "Analysis of the effect of impulse noise on multicarrier and single carrier QAM systems," *IEEE Transactions on Communications*, vol. 44, no. 2, pp. 145–147, 1996.

[26] G. Ndo, F. Labeau, and M. Kassouf, "A markov-middleton model for bursty impulsive noise: Modeling and receiver design," *IEEE Transactions on Power Delivery*, vol. 28, no. 4, pp. 2317–2325, 2013.

[27] D. Fertonani and G. Colavolpe, "On reliable communications over channels impaired by bursty impulse noise," *IEEE Transactions on Communications*, vol. 57, no. 7, pp. 2024–2030, 2009.

[28] J. Mitra and L. Lampe, "Convolutionally coded transmission over markov-gaussian channels: Analysis and decoding metrics," *IEEE Transactions on Communications*, vol. 58, no. 7, pp. 1939–1949, 2010.

[29] T. Shongwey, A. J. H. Vinck, and H. C. Ferreira, "On impulse noise and its models," in *Proceedings of the 18th IEEE International Symposium on Power Line Communications and Its Applications, IEEE ISPLC 2014*, pp. 12–17, IEEE, April 2014.

[30] V. V. Phan, S. G. Glisic, and D. D. Luong, "Packet-Length Adaptive CLSP/DS-CDMA: Performance in Burst-Error Correlated Fading Channels," *IEEE Transactions on Wireless Communications*, vol. 3, no. 1, pp. 147–158, 2004.

[31] M. Mushkin and I. Bar-David, "Capacity and coding for the Gilbert-Elliot channels," *IEEE Transactions on Information Theory*, vol. 35, no. 6, pp. 1277–1290, 1989.

[32] E. Cinlar, "An introduction to spatial queues," in *Advances in Queueing*, J. H. Dshalalow, Ed., CRC Press, Boca Raton, FL, USA, 1995.